

PIERCE GEOMETRY ELECTRON GUNS AS OFF-THE-SHELF NANOSECOND PULSED ELECTRON SOURCES

B.G. Birdsey^A, A.J. Alderman^A, A. Lurie^A, P. Hammond^A

^ASchool of Physics, University of Western Australia, Crawley, Australia.

Abstract

We have built and tested a new, simplified pulsed electron source delivering a pulse duration of ~ 10 ns. The design is based on an ordinary Pierce-geometry bent-wire electron gun and a 20 MHz function generator. The sine-wave signal driving the source has a peak-to-peak voltage of less than 4V. The design is not limited to this configuration and significantly better performance has been achieved using a purpose-built pulse generator.

Introduction

Our lab has been endeavouring to construct a sub-ns pulsed electron source to be used in a test-bench for time-resolved synchrotron experiments. In principle, pulsed electron systems are of broad interest in the physics community and technologies exist which can produce such pulses, but they are limited by special electron optical considerations, special surface preparation and the use of ultra-high-vacuum, highly specialized technical knowledge, and expense. Examples of such sources employ deflection plates (Samarin et al. 2004), modulation of grid potentials (Murray 1999), a combination of deflection plates and grid modulation (Khakoo 1984), RF-cavities (Weinfield 1976), and pulsed photoemission using fs laser pulses (Aeschlimann 1992).

The method presented in this work is competitive, but less restrictive compared to the methods referenced above. Our source does not require any special electron optical considerations, special equipment or electronics. As in the other voltage modulation schemes, the ultimate lower limit of pulse time is determined by the slew rate limit of the driving voltage supplies. The sensitivity of this source to the modulation voltage is similar to that demonstrated in (Murray 1999; Khakoo 1984) so in principle this source should be able to generate pulses at 350 ps reported in (Khakoo 1984) with similar driving electronics.

The pulsing is produced by a combination of factors, some of which are not yet fully understood. The primary factor is the modulation of the extraction voltage at the filament, similar to the grid-modulated scheme employed in (Murray 1999) (see figure 1). In the grid-modulated scheme, modulating the grid element also modulates the penetration of the anode potential through the grid. Below some sufficiently retarding grid voltage, no electrons will be passed through the grid. Above this threshold voltage the transmission efficiency rises rapidly, producing a sharp switch-like effect.

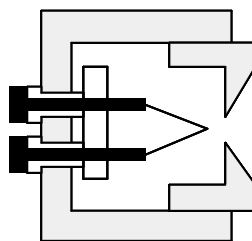


Figure 1 – Schematic of the Pierce-style cathode used in these experiments. The housing for the filament is 30mm in diameter and the anode (not pictured) would lie 2-4mm to the right of the grid element. The grid aperture is 2mm and the anode aperture is 1mm. The grid element itself is adjustable relative to the filament and has generally been set so that the tip of the filament lies at the tip of the cone-shaped cut-out in the grid. In this arrangement, the filament is completely enclosed.

Modulating the filament voltage in the opposite sense to the grid should produce an exactly analogous switch-like effect. On the contrary, the transmission efficiency has a strong peak vs. the filament voltage, as shown in figure 2. Two explanations have been tested: that decreasing the filament voltages causes the electrons to form a focus before the anode thereby decreasing the transmission through the anode, and that off-axis emission from the filament is being deflected

across the exit aperture of the anode. Both of these have been rejected after modelling of the filament-grid-anode system using CPO-3D (commercially available from www.electronoptics.com) failed to show any significant grid-voltage-dependent effect on the electron trajectories between the grid and anode. At this time, we suspect that electron space charge in the region near the filament may play some role.

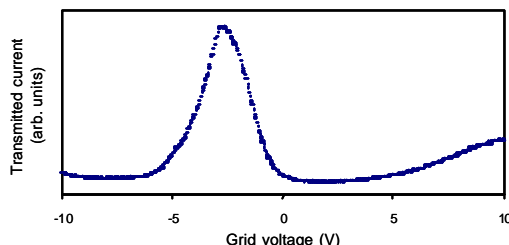


Figure 2 - Plot of the emission from the source as a function of filament voltage. In this case, the anode was located at 2 mm from the grid, the anode voltage was +240V, the grid voltage was ~0V, and the filament voltage was varied as indicated above.

This behaviour of the transmitted current as a function of filament voltage indicates two possible strategies for producing pulses. Toggling between -2.5 V and +2.5 V would produce a pulse of 16:1 signal to noise, at a repetition rate and pulse width limited by the switching speed of the voltage source. In another mode of operation, the source could be modulated between -7.5 V and +2.5 V, producing a pulse width that is limited by the maximum slew-rate of the voltage source. The TG220 20 MHz function generator used in the following experiment has a maximum measured slew rate of 1 V/ns, indicating that a temporal pulse width of ~5 ns should be able to be obtained using either of these techniques.

Materials and Methods

The experiment was conducted using basic equipment. The electron beamline (see figure 3) was contained in a 55 cm diameter cylindrical stainless-steel chamber with elastomer seals, pumped by a Varian V551 Navigator turbopump (550 l/s), producing a base of 10^{-6} Torr during this experiment. All signals in and out of the chamber were routed through double-ended BNC, MHV, or SHV connectors and all wires carrying pulses to and from the components inside the vacuum system were carried by (ordinary, not special UHV compatible) coax cable to minimise crosstalk between the pulsing and the electron pulse counting electronics.

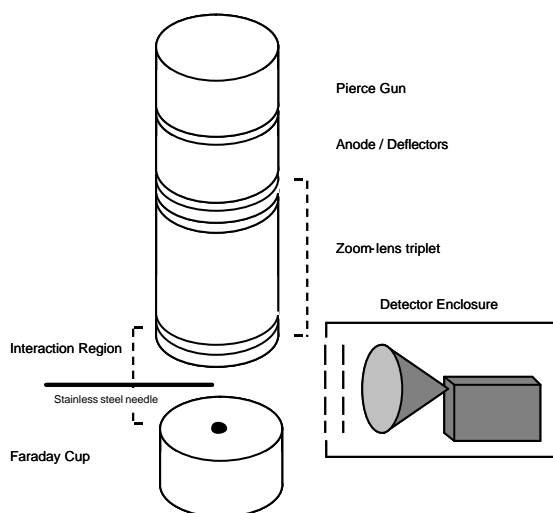


Figure 3 – Schematic of the apparatus. The beamline is arranged vertically, as shown. The components are shown roughly to scale. The outer diameter of the electron lens elements is 30mm, the inner diameter is 10mm, the distance between the lenses is ~2mm, the distance from the centre of the interaction to the detector enclosure is 20 mm, and the total distance to the front cone of the CEM is another 20mm. For the experiment described in here, the outer (grid) portion of the Pierce gun was at -2.7 V, the anode at +100V, the middle lens +12 V, and the interaction region +12 V. The Faraday Cup collector was biased to +192 V to prevent secondary electrons from escaping.

To obtain a large scattered signal from a compact target, the electrons were elastically scattered from a stainless steel surgical needle protruding into the interaction region. The scattered electrons were then detected by a Dr. Sjuets KBL25RS Channel Electron Multiplier (CEM) mounted 4 cm from the intersection of the needle and the electron beam.

The detector was mounted in an aluminium box to minimise cross-talk between the filament pulses and the collector of the CEM. The detector box also has grid covering the entrance to screen potentials inside the box from the interaction region as well as a retarding field grid between the entrance and the front cone of the CEM. The interaction region, the needle, the box housing the CEM, and Al-foil shielding around the interaction region were all held at the same potential, creating a field-free region between the interaction region and the entrance to the detector box.

The pulse is injected into the filament using a simple electronic circuit (figure 4) that isolates the pulsing signal from the current supply driving the bent wire filament. The essential design elements of this circuit are that the filament supply should be floating on the voltage supplied by the pulsing unit and that there should be proper termination of pulses at the outputs of the current supply so that they will not reflect from these un-balanced connections. Another significant design consideration in this experiment was minimisation of cross-talk between the pulsing electronics and the CEM pulse detection electronics. Such cross-talk or “noise” is significantly troublesome in that it is in synchrony with the incoming pulse and can (if not handled properly) mask any actual signal from being detected. The driving pulses are relatively strong (a signal several volts in magnitude, varying on nano-second timescales). The most effective method for dealing with this problem was the elimination of all ground-loops and virtual ground-loops between the pulsing and detection electronics. This reduced the measured cross talk signal (the maximum peak-to-peak voltage at the input to the Amplifier/Discriminator when there is no voltage across the CEM) to 200-700 μV -pp. This is enough noise to cause a modulation of the detected count rate by the voltage of the cross-talk signal at the input to the Amplifier/Discriminator, which can be thought of as the cross-talk signal shifting the threshold of the CEM’s discriminator as a function of time. To counteract this effect it is necessary that the average pulse height out of the CEM be $\gg 700 \mu\text{V}$. In practice, this means for detection of elastically scattered electrons, the electron current in the target region must be kept at levels significantly below 1 nA and that the CEM gain must be at or above single pulse saturation (where increasing the gain of the CEM no longer increases the measured counting rate).

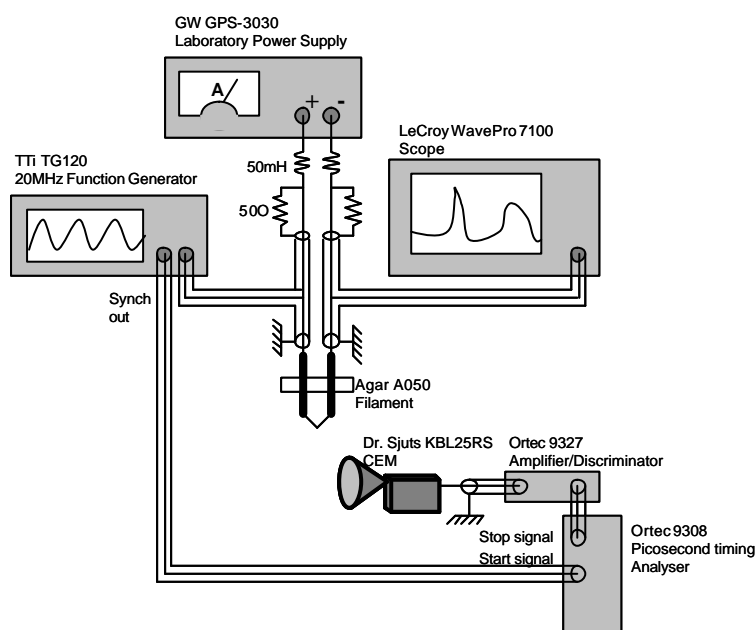


Figure 4 – Schematic of the electronic instrumentation. As mentioned in the text, great care was taken to isolate the pulse generation from the electron detection and to isolate the current supply from the pulse generation. The pulse signal is generated in the function generator and splits at the 1st T-intersection. The circuit at the “+” terminal of the power supply isolates the power supply and prevents reflections. The other half of the pulse travels through the filament. Half of this transmitted pulse then goes to the Scope and half is absorbed at the “-” terminal of the current supply. On the Pulse detection side, the raw pulse from the CEM is amplified by the matched Amplifier / Constant-Fraction Discriminator before being registered by the 65,536 channel timing analyser.

Results and Discussion

By eliminating as much cross-talk as possible and operating the CEM at optimal performance, we have been able to detect elastically scattered electron pulses from the stainless steel needle as short as ~ 7 ns FWHM (see the pulse at 59 ns in figure 5). In this case, a 10 MHz sine wave was used to drive the pulsing of the filament as it has relatively few higher harmonics that could excite resonances between the pulse generation and pulse counting circuits. The triangle wave and square wave are too distorted at 10 MHz and the resultant detected signal is completely dominated by noise.

The pulse generation system was configured to give maximum throughput when the input to the filament was grounded. This does not, of course correspond to 0V bias at the tip of the filament, as it specifies the voltage at one side of the filament and there is a voltage drop across the filament due to the resistive heating. In the figure, the measured driving voltage has been shifted to account for the unknown electron time-of-flight so that a 0V reading on the oscilloscope corresponds to the observed electron pulses. As mentioned in the figure, the observed count rate still contains some electronic noise when using the function generator to drive the pulsing. Both we and the group of Tim Reddish at the University of Windsor have been able to use purpose-built pulsing units to produce clean, and sharply defined square wave pulses. We have been able to produce well defined pulses with widths below 10 ns.

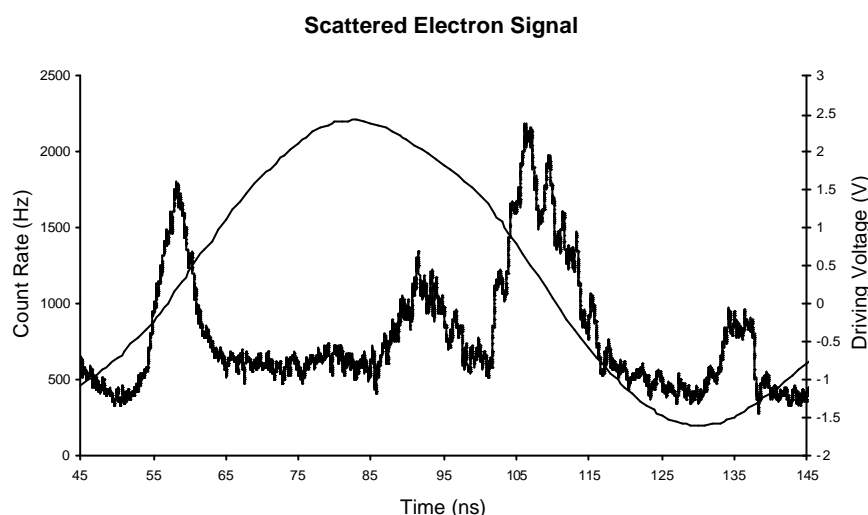


Figure 5 – Output electron pulses and artefacts from electronic noise. The jagged line with peaks at roughly 59 ns, 90 ns, etc. is the measured count rate in the channel electron multiplier viewing the interaction region. The measured count rate is composed of counts from actual elastically scattered electrons (at 59 ns and 110 ns) as well as some residual noise (at 90 ns and 135 ns). The noise was identified by measuring the apparent count rate in each peak while a retarding potential blocked the entire electron signal. The pulsed gun was configured to “fire” when the driving voltage was at 0 V with respect to the common earth of the apparatus.

Conclusions

It is possible to obtain experimentally useful nanosecond-scale electron pulses using a Pierce-geometry cathode and an inexpensive 20MHz function generator. The major obstacle is the cross-talk between the nanosecond-scale pulse driving the electron emission and the input to the detection circuit. We have identified and implemented several methods for reducing this source of noise. This technology has already been used by another group to modify an existing electron gun to make short pulses and obtain scientific results (see Tessier WC0328, this conference proceedings). Much better performance has been demonstrated with purpose-built pulsing units, including almost complete suppression of artefacts from cross-talk in measurements similar to those in figure 5.

Acknowledgements

We wish to acknowledge the University of Western Australia and the Australian Research Council for their support and generous funding of this, and other experimental work.

References

- Aeschlimann, M. *et al.* (1995). A picosecond electron gun for surface analysis. *Rev. Sci. Instrum.*, v 66, p 1000.
- Khakoo, M.A. and Srivastava, S.K. (1984). A compact high current pulsed electron gun with subnanosecond electron pulse widths. *J. Phys. E : Sci. Instrum.*, v 17, p 1008.
- Murray, A. and Hammond, P. (1999). A novel spectrometer combining laser and electron excitation and deflection of atoms and molecules. *Rev. Sci. Instrum.* v 70, p 1939.
- Samarin, S., *et al.* (2004). Secondary-electron emission mechanism of LiF film by (e, 2e) spectroscopy. *Surface Science*, v 548, p 187.
- Weinfeld, M. and Bouschoule, A. (1976). Electron gun for generation of subnanosecond electron packets at very high repetition rate. *Rev. Sci. Instrum.* v 47, p 412.